

EXPERIMENTAL RESEARCH ON THE CAPACITY OF BRIDGE SHEAR KEYS

Stergios A. Mitoulis^{1*}, Ioannis A. Tegos², Andreas Malekakis³

¹Civil and Environmental Engineering, Surrey University
e-mail: s.mitoulis@surrey.ac.uk

^{2,3}Aristotle University of Thessaloniki, Laboratory of Reinforced Concrete and Masonry Structures,
email: itegos@civil.auth.gr

Keywords: Bridge, Shear key, Design, experiment, effective width.

Abstract. *Conceptual design of bridges has evolved rapidly during the last ten years and new, efficient and cost effective design schemes have been introduced in practice. Use of shear keys, as an active seismic link, is not prohibited in current codes. However, the major concern of having the shear keys damaged one-by-one due to their asynchronous participation still remains an open issue. As such, shear keys are typically used to prevent potential span unseating. Shear keys, also known in European literature as seismic links or stoppers, are stub RC structural elements. A capacity design procedure is provided for these elements, to safeguard the support of the deck. Design of shear keys engineering is an open issue in contemporary bridge. Current state-of-the-art deals with the efficient use of reinforcements, while practitioner engineers dealt with the seismic role of these elements and have proposed different materials for the design of stoppers and/or different reinforcement materials, since sacrificial shear keys can respond as structural fuses to limit the demand of the piers. Shear keys, whether they receive seismic actions or not -the last referring to the case in which keys are utilized to avoid the common unseating of the spans- have peculiar response and unconventional reinforcement requirements due to their loading. Simultaneously, their geometry and size is restricted due to bridge's esthetics. Hence, stoppers are relatively small and stub concrete "blocks", which are expected to receive reliably and safely large pounding forces. In this framework, two alternative reinforcement layouts with transverse hairpin bars were assessed. The efficiency of the proposed reinforcement was assessed by comparing the above rebar with the state-of-practice shear key reinforcements. The required hairpin reinforcement ratio was then evaluated through an analytical procedure that accounted for the relation between the reinforcement hairpin ratio vs the capacity of the shear keys. The procedure indicated the most appropriate reinforcement ratio for a required capacity of the stopper. The study proposes the reinforcement of the stoppers with additional diagonal rebar. Conclusions are drawn based on the analytical models and the experimental campaign.*

1 INTRODUCTION

Conceptual design of earthquake resistant bridges has evolved rapidly during the last ten years. New design concepts based on hybrid earthquake resisting concepts [1][2][3][4][5], seismic isolation [6][7], integral and semi-integral lateral resisting systems [8][9] have been introduced in modern bridge designs. Within this evolution, a noiseless but practically sustainable philosophy has been established. The philosophy is based on the design of bridges in which serviceability movements of the deck are tackled with isolation bearings, while central piers that are less susceptible to constraint movements due to creep and shrinkage, are expected to receive seismic loading and provide ductility to the structure. This concept is deemed to be enhanced by the use of seismically active shear keys, in the sense that appropriate gaps may be left between the superstructure and the bents to provide space for deck's "breath" (i.e. contraction and expansion), while in case of large longitudinal loading, the shear keys may restrain movements.

Shear keys serve to restrain the deck displacements in either the longitudinal or transverse direction of the bridge. These devices are typically reinforced concrete blocks provided at each bearing location. They have found to be more effective in protecting bearing vulnerability in the transverse direction of the bridge [10]. However, Eurocode 8-2 (2005) [11] allows the use of the so-called seismic links (shear keys) also in the longitudinal direction, as means to reduce the seismic displacements of the deck and to minimize the potential of span unseating in case insufficient seat lengths are used [12]. Many different designs have been proposed in the past for the shear keys. Ghosh et al [13] have tested rigid stopper devices, yielding stoppers, steel restrainers, and superelastic shape memory alloy (SMA) shear keys. A study on the seismic performance of girder bridges equipped with bi-directional energy-dissipating sacrificial devices have been performed by Kwang et al. [14]. Different design approaches of these elements have been proposed in the past by other researchers [15] [16] [17]. Current codes [11] [18] [19] [20] place the focus on the prevention of falling off the superstructure and no attention is given to the prevention of the failure and the reinforcements of the stoppers itself. However, further advances on appropriate methods and devices of preventing 'dislodgement' or 'unseating' of the superstructure in the event of severe ground shaking have been established. These ideas can be used in economical earthquake resistant design of bridges as stated by [21][22]. In that case stoppers must be appropriately designed. Correct design of stoppers should include not only reinforcements, as shear keys shall be designed for the axial and shear forces associated with the column's overstrength moment including the effects of overturning, but also a correct estimation of the effective width that should be taken into account when calculating the capacity of the pier cap beam especially in bridges with hammerhead piers.

In this framework, two alternative reinforcement layouts with transverse hairpin bars were assessed. The efficiency of the proposed reinforcement was assessed by comparing the above rebar with the current/state-of-practice shear keys reinforcements based on Eurocode 8-2 [11] and other researchers [23][24] that is based on the sliding shear and the diagonal tension. The required hairpin reinforcement ratio was then evaluated through an analytical procedure that accounted for the relation between the reinforcement hairpin ratio vs the capacity of the shear keys. The procedure indicated the most appropriate reinforcement ratio for a required capacity of the stopper. The study proposes the reinforcement of the stoppers with additional diagonal rebar. Conclusions are drawn based on the analytical models and the experimental campaign.

2 TYPICAL EXAMPLES OF SHORT AND VERY SHORT STRUCTURAL ELEMENTS-THE PROBLEM OF EFFECTIVE WIDTH

Figure 1 shows different typical cases of short cantilevers used in practice. Such structural elements are met in most bridge structures either in end supports (Figure 1a), longitudinal stoppers installed at the abutments (Figure 1b) or intermediate supports of beams above the piers (Figure 1c). In that case the effective width of the structural elements should be determined, as the calculation of the effective width based on codes does not cover such cases for two distinct reasons: (a) the loads imposed at the short elements illustrated at Figures 1a, b and c are concentrated and as such the typical calculation of the effective width that correspond to distributed loads is not considered to be appropriate and (b) loading of these elements is either static, dynamic or pounding-type (extremely dynamic) loading that may lead to different effective widths. For example the imposition of load on the shear keys is extremely dynamic.

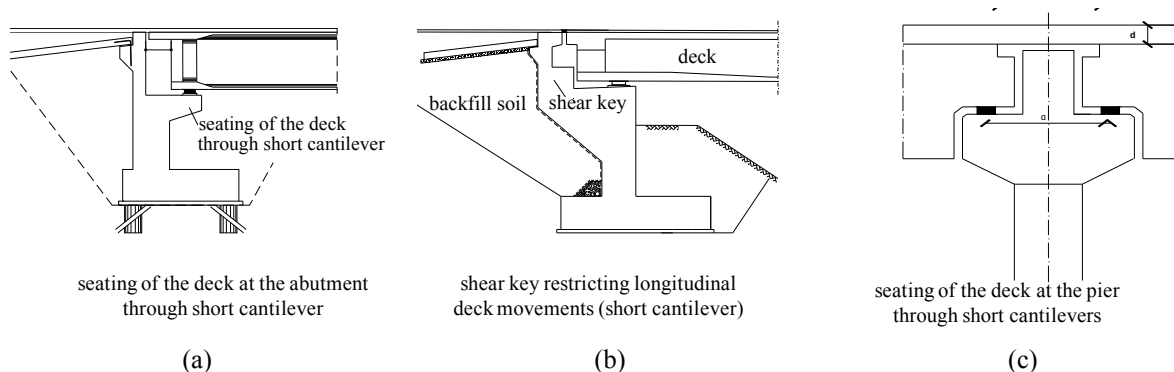
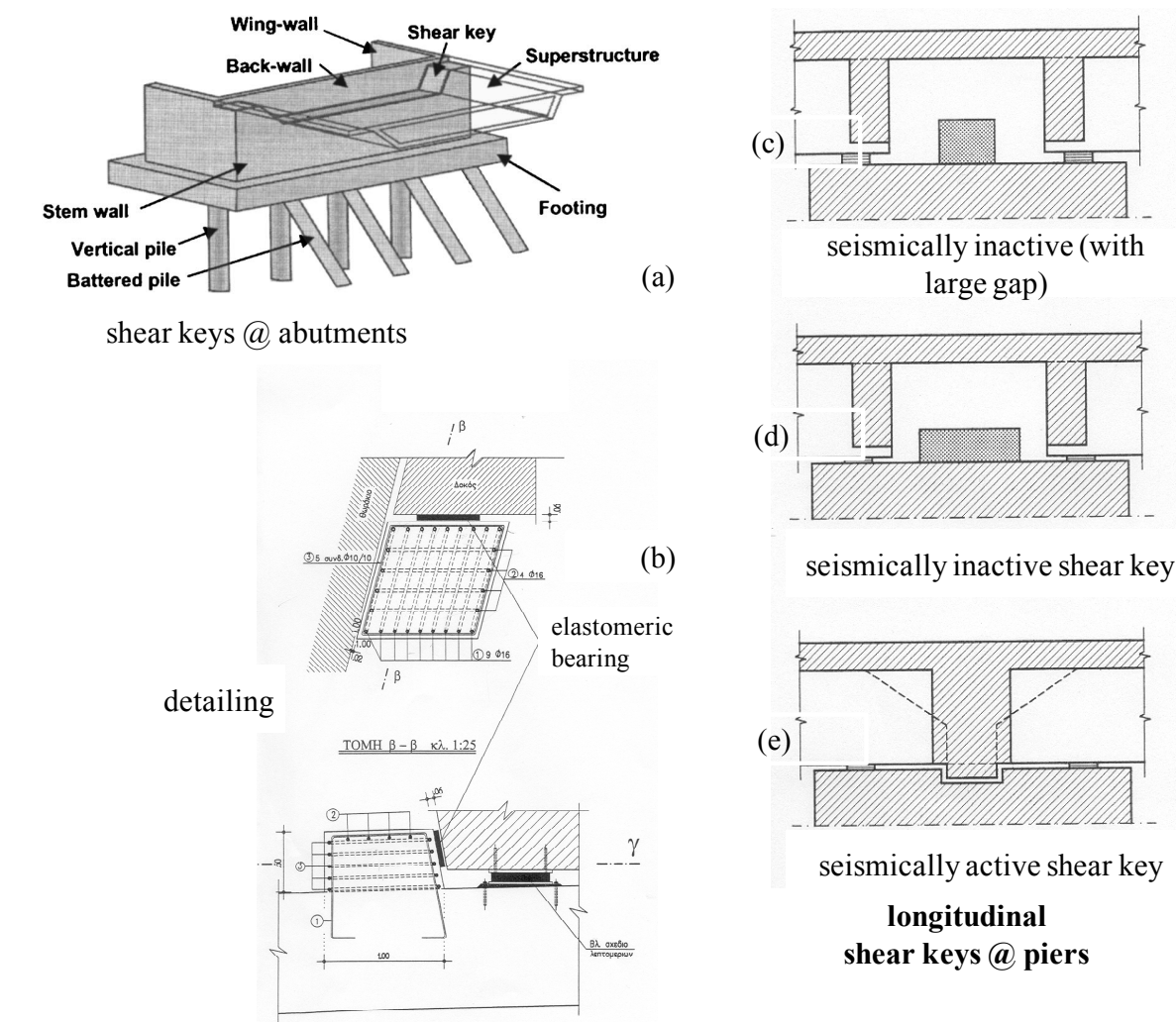


Figure 1: Three typical cases where short cantilevers are used in practice and their effective width should be calculated, (examples of short and very short cantilevers).

Figure 2 illustrates shear keys at the abutments and at the piers. Use of shear keys is common at the abutments. Figure 2a shows a typical shear key that restrains transverse movements at the abutments, while Figure 2b shows in detail the reinforcements used at such shear keys. An elastomeric bearing is interjected between the deck and the shear keys in order to increase the duration of pounding and hence to reduce effectively the magnitude of potential pounding forces during an earthquake. High reinforcement ratios, including both longitudinal and transverse-hairpin bars, cause congestion of steel within the shear keys. Another issue is the structural joint left between the shear key and the cap-beam, as the cap beam is casted prior to the construction of the shear keys.

Figure 2c, d and e show the use of shear keys at bridge piers. Two different types of shear keys can be found in contemporary bridges: (a) seismically inactive shear keys shown in Figures 2c and d having a large gap between the superstructure and the piers. Seismically inactive shear keys are typically used to prevent span unseating of the deck. (b) Seismically active shear keys shown in Figure 2e. Active shear keys are designed to allow for serviceability deck movements, due to creep, shrinkage and thermal effects, while during an earthquake shear keys transmit the seismic actions to the piers.



dinal dimension of the specimens was 600mm. This paper emphasized on the second type of shear keys, which are the most common ones met in bridge structures.

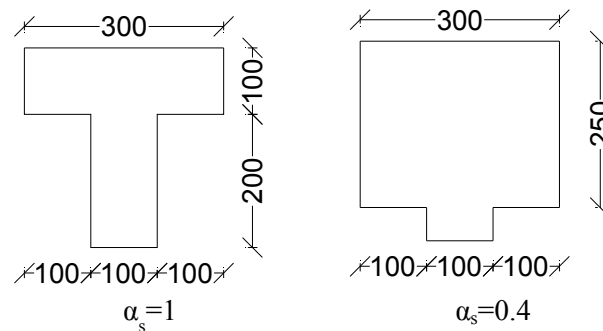


Figure 3: Cross sections of the specimen (a) short cantilever with shear ratio $\alpha_s=1$ and (b) very short cantilever with $\alpha_s=0.4$ referring to shear keys.

3.2 Loading

Loading is shown in Figure 4. The shear keys are considered to be extended along the total transverse width of the seating beam. Different types of loading were imposed to the specimen. The specimens were initially being loaded to the total length that is 600mm. This case represented the total capacity of the shear key and corresponds to the maximum load that the shear key can receive. This loading represents the ideal case that a bridge is subjected to longitudinal seismic motion, i.e. no out of plane rotations of the deck are expected. Then different lengths (see dimension α in Figure 4c) of the shear key were tested to identify different effective widths of the shear key. Additionally, different loading areas we also tested, as on the one hand the total load was applied in the central part of the specimen, as shown in Figure 4c and 4d, while specimens having been loaded at their ends were also tested (as shown in Figure 4e). Short cantilevers having shear ratio $\alpha_s=0.4$ as well as flexural shear keys having shear ratio $\alpha_s=1$ were tested. To take into account the fact that not all of the height of the shear key is loaded, the load was applied along different widths (distance b in Figure 4c) ranging from 50mm to 100mm. Loading of the shear keys is not applied to all of its height due to the fact that between the pier cap and the superstructure a bearing with a considerable height (typically between 50 to 200mm including the preparatory concrete slabs) is interjected and raises the level of the superstructure with respect the pier-cap. Hence, the shear key, which is fixed at the pier cap, receives at its upper part the loading of the superstructure. To model this effect, i.e. the potential loading of the shear keys at different heights, different widths of loading were applied to the specimen (width of loading b is shown in Figure 4c). Part of the results of the extended experimental campaign is shown in this paper. Emphasis was placed on the case where $\alpha=150$ mm and $b=50$ mm, while both the outcomes of the central (Figure 4c and 4d) and end loading (shown in Figure 4e) are given.

Effective width was calculated by comparing the capacity of the shear keys when the total length (600mm) of the shear was loaded to the one that was experimentally extracted when a smaller loading width $\alpha=150$ mm was adopted. The latter case, i.e. the loading of 150mm of the specimen, yielded a capacity that was smaller than the one found for the $\alpha=600$ mm loading width. However, the first load, which corresponds to $\alpha=150$ mm was not $600/150=4$ times smaller due to the development of the effective width of the shear keys. Hence, additional loading was deemed to be due to the effective width. The loading shown in Figure 4c and d are expected to reveal what is the effective width of the stoppers when both sides of the shear key are activated, while the loading shown in Figure 4e corresponds to the case that the shear

key is expected to be assisted by one-side effective widths and corresponds to the case where end sacrificial keys are used, i.e. shear keys installed at the ends of the cap-beams.

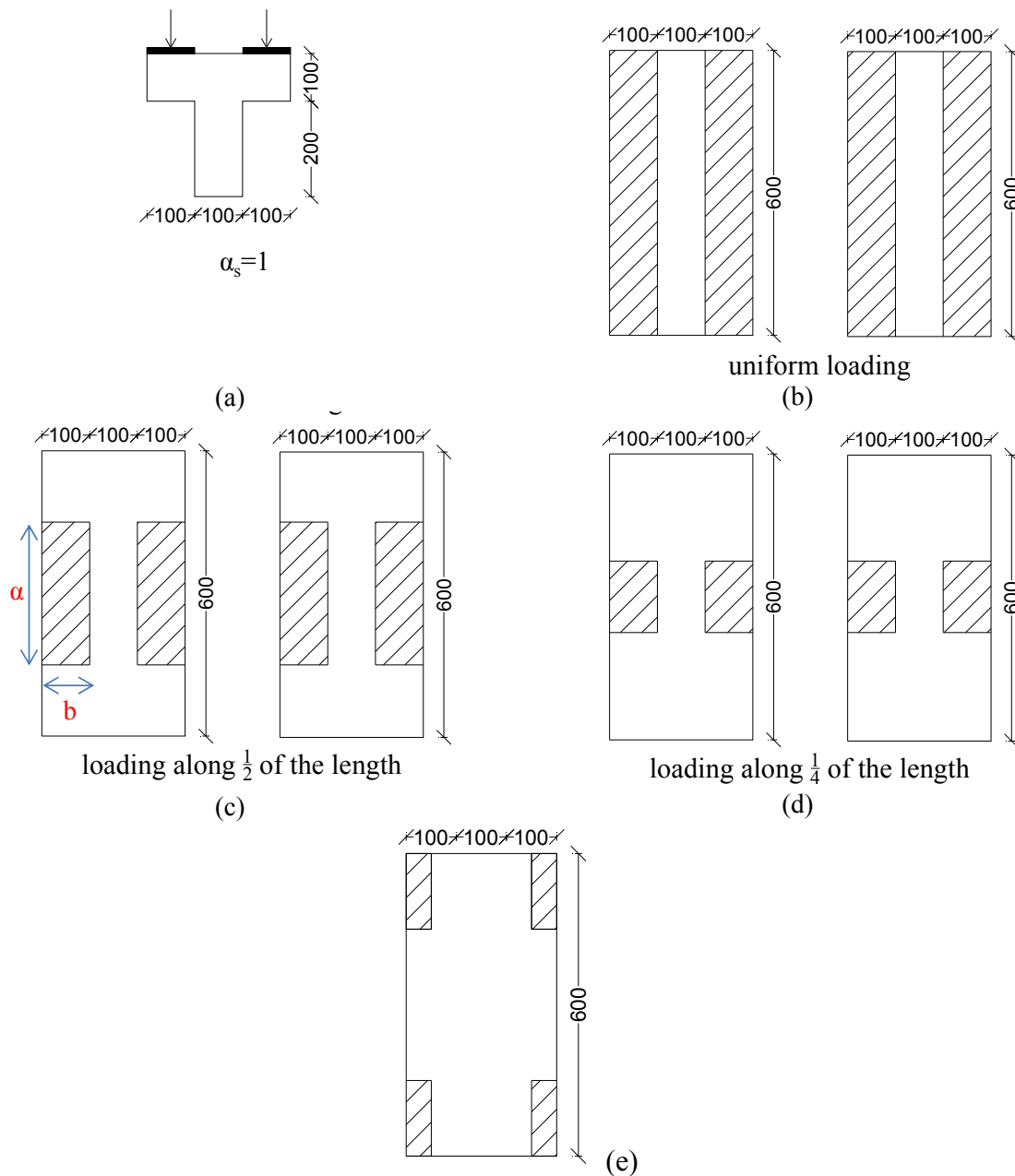


Figure 4: The loading of the specimens: (a) cross section of the specimen and loading; (b) uniform loading to obtain the maximum shear key capacity, (c) loading at half ($\frac{1}{2}$) of the specimen's length, distances α and b of the loading are shown in this figure, (d) loading at a quarter ($\frac{1}{4}$) of the specimen's length; (e) loading at the quarters ($\frac{1}{4} + \frac{1}{4}$) ends of the specimen.

Figures 5 to 10 illustrate different designs attempted for the shear keys. Different tests were aimed at identifying what are the most efficient reinforcements in enhancing both the capacity and the effective width of the shear key. A total of twelve different tests are illustrated in this paper. Figure 5 shows a picture of the specimen reinforcements. Thirteen hairpin shear reinforcements having a diameter 8mm (13Ø8) were used in this specimen, while no significant longitudinal reinforcements were used in this case. Five “floors” of reinforcements

were used in the height of the stopper to enhance the capacity of the shear key. Figure 6 illustrates the reinforcement layout of a different specimen having both hairpin reinforcements and strong longitudinal (along the 600mm length of the specimen) reinforcements. Figures 6 to 11 illustrate all the different specimens tested in the laboratory. Reinforcement layout and geometries are also given in detail.



Figure 5: Sample of the reinforcements of the shear keys.

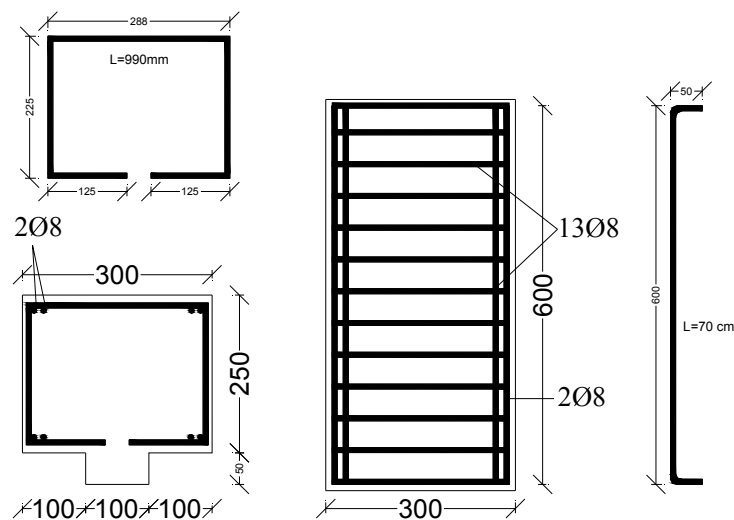


Figure 6. Reinforcement layout and geometry of specimen 1 (Specimen code 3.1 - loading at 1/4 of the length).

4 RESULTS

Figures 12 to 17 and the embedded tables illustrate the results of the experimental campaign. The maximum load recorded at all the tests was recorded. The black lines illustrate the maximum capacity of the shear keys reached when the loading was uniform along the longitudinal 600mm length of the specimen. The gray lines illustrate the capacity of specimen with identical geometries and reinforcements, but for a loading corresponding to a part of the longitudinal dimension $l=600\text{mm}$ of the specimen, i.e. $l/4$ at the mid-span (central part of the specimen) or $l/4+l/4$, i.e. the quarters of the specimen's ends as shown in Figure 4e.

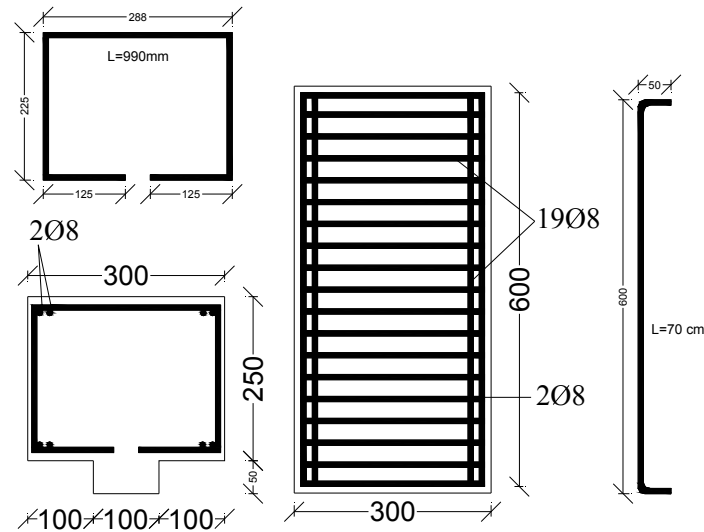


Figure 7. Reinforcement layout and geometry of specimen 2 (Specimen code 3.2 - loading at 1/4 of the length)

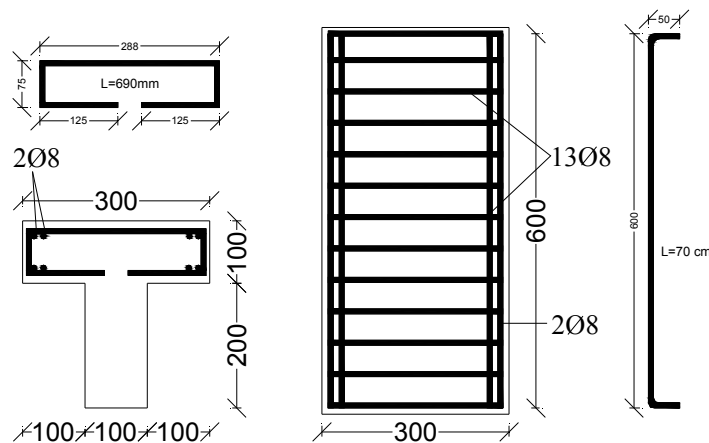


Figure 8. Reinforcement layout and geometry of specimen 3 (Specimen code 3.3 - loading at 1/4 of the length).

Figure 12 shows the recorded capacity vs displacement of the first specimen. Strong hair-pin reinforcements were used in this specimen. The first column of the table under the figure shows the loading length, which is either the total length of the specimen (black line), i.e. 600mm or a quarter of the specimen's length (gray line), i.e. 150mm. The second column of the table shows the capacity per length of the specimen, i.e. the first column divided by 0.6m. This quantity is meaningful for the first loading of the specimen, as in the second loading type both the 1/4 plus the effective width of the specimen are receiving the load. The third column indicates the prospected capacity of the specimen. This capacity is meaningful only for the second loading (at 1/4) of the specimen and shows what would be the prospected capacity of the specimen in case no effective width had participated in the total capacity of the specimen. Hence, this value is the outcome of the capacity per length of the specimen (column 2) multiplied by 150mm, which is the loading width. Accordingly, column 5 shows the additional effective length, which is the additional capacity (588.60 minus 370.25kN based on the results above) divided by 2468.32kN/m. Hence, the width of loading (i.e. 150mm) plus the addition

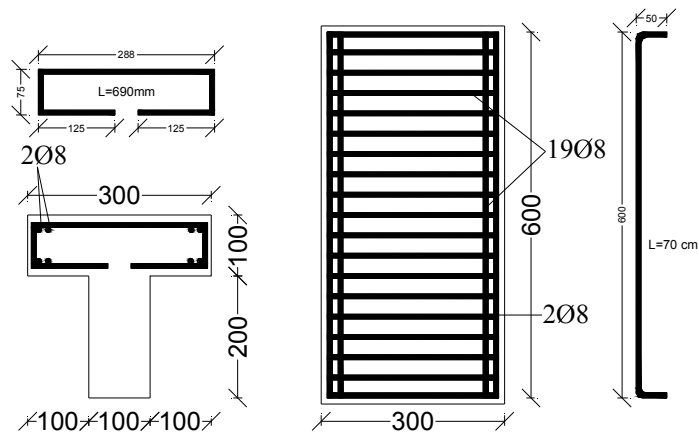


Figure 9. Reinforcement layout and geometry of specimen 4 (Specimen code 3.4 - loading at 1/4 of the length).

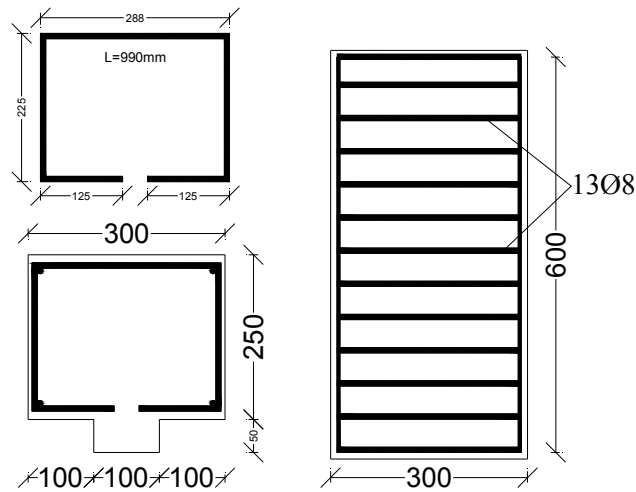


Figure 10. Reinforcement layout and geometry of specimen 5 (Specimen code 3.5 - loading at 1/4 of the length).

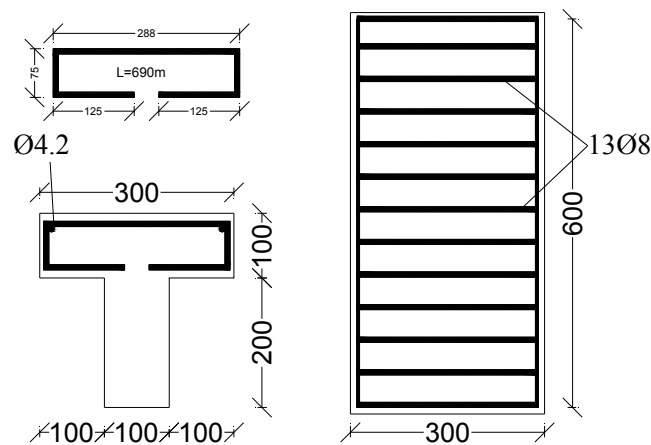
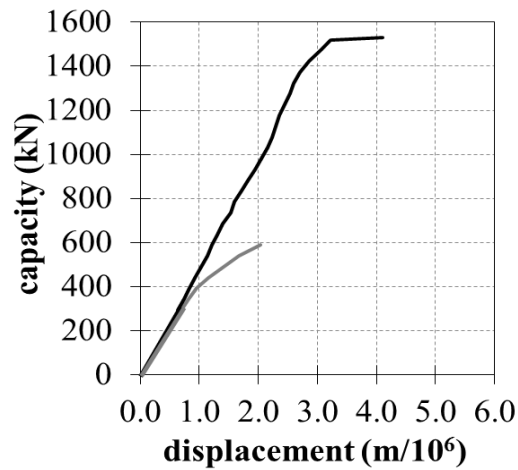
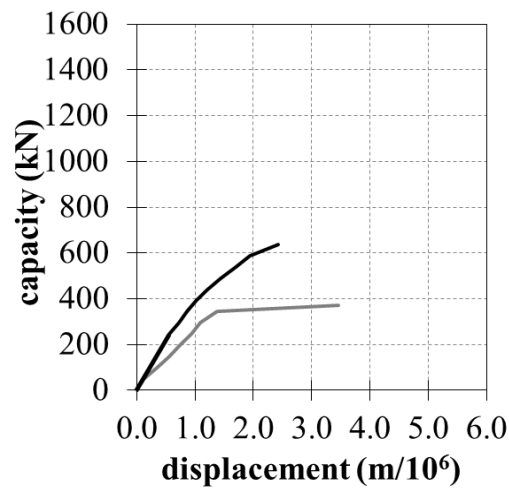


Figure 11. Reinforcement layout and geometry of specimen 6 (Specimen code 3.6 - loading at 1/4 of the length).



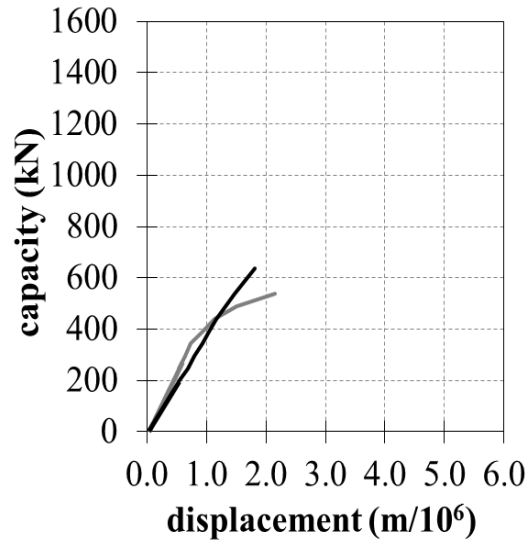
loading length α (mm)	capacity (kN)	capacity per length (kN/m)	prospected capacity (kN)	additional effective length (m)	additional effective length at each side (m)	prospected angle of distribution (deg)
600mm	1530.36	2468.32	-	-	-	-
150mm	588.60	-	370.25	0.088	0.044	41.5

Figure 12. Capacity vs displacement of the 1st specimen under loading at l and at l/4 mid-span.



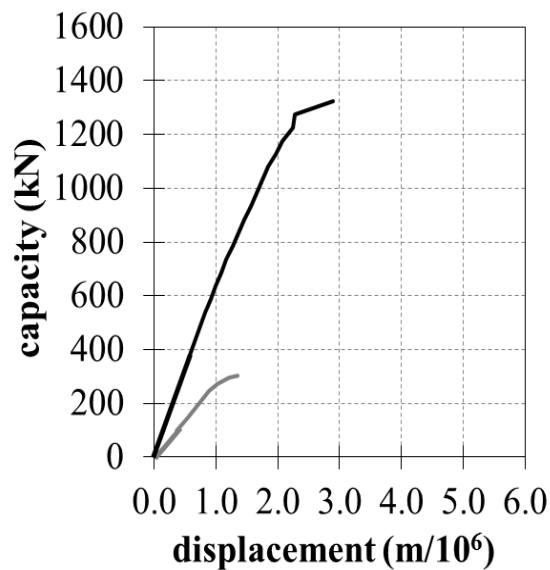
loading length α (mm)	capacity (kN)	capacity per length (kN/m)	prospected capacity (kN)	additional effective length (m)	additional effective length at each side (m)	prospected angle of distribution (deg)
600mm	637.65	1028.47	-	-	-	-
150mm	372.78	-	154.27	0.212	0.106	64.8

Figure 13. Capacity vs displacement of the 2nd specimen under loading at l and at l/4 mid-span.



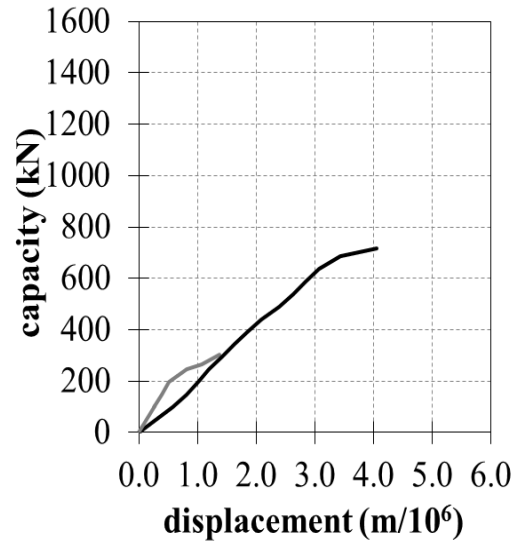
loading length α (mm)	capacity (kN)	capacity per length (kN/m)	prospected capacity (kN)	additional effective length (m)	additional effective length at each side (m)	prospected angle of distribution (deg)
600mm	637.65	1028.47	-	-	-	-
150mm	539.55	-	154.27	0.375	0.187	75.1

Figure 14. Capacity vs displacement of the 3rd specimen under loading at l and at l/4 mid-span.



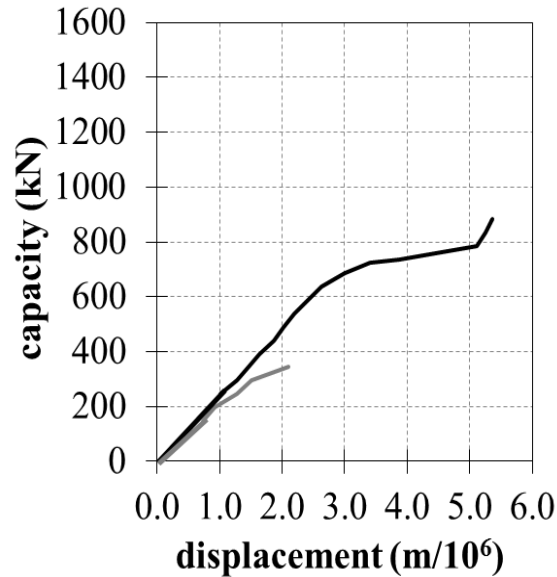
loading length α (mm)	capacity (kN)	capacity per length (kN/m)	prospected capacity (kN)	additional effective length (m)	additional effective length at each side (m)	prospected angle of distribution (deg)
600mm	1324.35	2136.05	-	-	-	-
150mm	304.11	-	320.41	-0.008	-0.004	-4.4

Figure 15. Capacity vs displacement of the 4th specimen under loading at l and at l/4 end part.



loading length α (mm)	capacity (kN)	capacity per length (kN/m)	prospected capacity (kN)	additional effective length (m)	additional effective length at each side (m)	prospected angle of distribution (deg)
600mm	0.00	0.00	-	-	-	-
150mm	716.13	-	304.11	0.000	0.000	0.8

Figure 16. Capacity vs displacement of the 5th specimen under loading at l and l/4 end part.



loading length α (mm)	capacity (kN)	capacity per length (kN/m)	prospected capacity (kN)	additional effective length (m)	additional effective length at each side (m)	prospected angle of distribution (deg)
600mm	0.00	0.00	-	-	-	-
150mm	882.90	-	343.35	0.000	0.000	0.7

Figure 17. Capacity vs displacement of the 6th specimen under loading at l and l/4 end part.

al effective length calculated in column 5 results in the effective length of the specimen that receives the loading. Since, the loading in the specimen's mid-span the additional effective length (88mm) is extended at both sides of loading width (150mm). Hence, the additional width that participates in receiving the loading at each side is $88\text{mm}/2=44\text{mm}$ and this is given in column 6 of the table. Based on the result given in column 6 and taking into account the geometry of the specimen it is possible to calculate the inclination of the crack that caused the failure of the specimen. This angle also indicates the effective length of the shear key. This angle is given in codes equal to 45 deg, however, the experimental campaign revealed that this angle can vary based upon the loading type -uniform or concentrated- the geometry of the specimen, i.e the shear ratio, and the reinforcement of the shear key. Specimen 1 to 3 were found to have a clear increase in their effective width, while the angles calculated are ranging from 41.5 deg to 75.1 deg, showing that the reinforcements in that case increased the effective width of the shear keys. Additionally, the loading of the specimen at the mid-span was identified to be a favorable loading condition. Contrarily, the specimens 4 to 6 illustrate a poor distribution of action, as it seems that no additional length of the specimens is participating in receiving loading. Prospected angles of load distribution were found to be either negligible $\sim 1\text{deg}$ or even negative, showing that one the one hand the loading at the end of the specimen is an unfavorable loading condition and, on the other hand, the reinforcements in these specimen failed to enhance both the capacity and the of the shear keys effective width of the shear keys.

Elaboration on the experimental outcomes, which was also complemented by past experiments, yielded similar force-displacement diagrams. The following analytical equation was derived representing the effective width of shear keys:

$$b_{\text{eff}} = b_0 + \lambda \cdot \alpha \cdot l_k \quad \text{eq. 1}$$

where b_0 is the width of the loading, α is the shear ratio equal to l_k/d_c where l_k is the distance of the loading input with respect the fixing joint of the stopper and h_c is the height of the shear key, λ is the coefficient that was calculated based on the experimental campaign that is equal to 1.6 for cantilevers with $\alpha \geq 1$, while equals 1.4 for short and very short cantilevers, i.e. when $\alpha < 1$.

5 CONCLUSIONS

This paper aims at shedding light on the conceptual design of bridges by utilizing seismically active shear keys that restrain longitudinal seismic movements of the deck, while providing adequate gaps to let the bridge “breath” under thermal, creep and shrinkage movements. Alternative designs of shear keys with different reinforcements and different loading patterns were introduced in order to identify on the one hand the efficiency of reinforcement layouts on the capacity of the keys and the prospected effective width of the shear keys. Outcomes of an extended experimental study were illustrated with emphasis placed on keys having a low shear ratio $\alpha_s=0.4$. The following conclusions were drawn:

- The capacity of the shear keys can be enhanced when utilizing main longitudinal reinforcements, additional (secondary) longitudinal reinforcements set at levels parallel to the one of the main reinforcements and long hairpin shear reinforcements.

- Secondary longitudinal reinforcements were found to increase the effective width of the shear key, which is a desirable effect as keys are typically loaded by concentrated loads.
- The distribution of the load does not follow the known 45 degrees mode, which means that a revision is needed in case shear keys are loaded under concentrated loads, especially when the load is not central.

REFERENCES

- [1] S.A. Mitoulis, Seismic design of bridges with the participation of seat-type abutments, *Engineering Structures*. 44, pp. 222-233, 2012.
- [2] S.A. Mitoulis, I.A. Tegos, Two new earthquake resistant integral abutments for medium to long-span bridges, *Structural Engineering International: Journal of the International Association for Bridge and Structural Engineering (IABSE)*, 21 (2), pp. 157-161, 2011.
- [3] S.A. Mitoulis, I.A. Tegos, An unconventional restraining system for limiting the seismic movements of isolated bridges, *Engineering Structures*. 32(4), pp. 1100-1112, 2010.
- [4] S.A. Mitoulis, I.A. Tegos, Connection of bridges with neighbour-hooding tunnels, *Journal of Earthquake Engineering (JEE)*, 1559-808X, 14(3), pp. 331-350, 2010.
- [5] S.A. Mitoulis, I.A. Tegos, Restrain of a seismically isolated bridge by external stoppers, *Bulletin of Earthquake Engineering*, 8(4), pp. 973-993, 2010.
- [6] I.G. Buckle, M.C. Constantinou, M. Dicleli, and H. Ghasemi, Seismic Isolation of Highway Bridges. *Special Report MCEER-06-SP07*, Multidisciplinary Center for Earthquake Engineering Research, Buffalo, NY, 171pp, 2006.
- [7] M.C. Kunde and R.S. Jangid, Effects of Pier and Deck Flexibility on the Seismic Response of Isolated Bridges. *Journal of Bridge Engineering*, 11(1), 2006.
- [8] M. Arockiasamy, N. Butrieng, M. Sivakumar, State-of-the-art of integral abutment bridges: Design and practice. *ASCE Journal of Bridge Engineering*. 9(5):497-506, 2004.
- [9] S. Arsoy, J.M. Duncan, R.M. Barker. Behavior of a semiintegral bridge abutment under static and temperature-induced cyclic loading. *ASCE Journal of Bridge Engineering*, 9(2): 193-199, 2004.
- [10] J.E. Padgett, R. DesRoches, Three-Dimensional Nonlinear Seismic Performance Evaluation of Retrofit Measures for Typical Steel Girder Bridges, *Engineering Structures*, 30(7), pp. 1869-1878, 2008.
- [11] EN 1998-2. Eurocode 8: *Design of structures for earthquake resistance*, Part 2: *Bridges*., 2005
- [12] M.T.A. Chaudhary, M. Abe, Y. Fujino, Investigation of a typical seismic response of a base-isolated bridge. *Engineering Structures*, 24(7), 945-953, 2002.
- [13] G. Ghosh, Y. Singh, S.K. Thakkar, Seismic response of a continuous bridge with bearing protection devices, *Engineering Structures*, 33(4), pp. 1149-1156, 2011.

- [14] K-I. Cho, S.-H. Kim, M.-S. Choi and J.-Y. Lim, A Study on Seismic Performance of Girder Bridges Equipped with Bi-Directional Energy-Dissipating Sacrificial Devices, *Steel Structures*, 8, pp. 59-65, 2008.
- [15] M. Saiidi, E.A. Maragakis, S. Feng, An evaluation of the current Caltrans seismic restrainer design method. *Report No. CCEER-92-8*. Reno (NV): Civil Engineering Department, University of Nevada; 1992.
- [16] [7] Fenves G, DesRoches R. Response of the Northwest Connector in the Landers and Big Bear earthquakes. Report No. UCB/EERC-94/12. Berkeley (CA): University of California; 1994.
- [17] L.G Selena, L.J. Malvar, R.J. Zelinski, Bridge retrofit testing: hinge cable restrainers. *ASCE Journal of Structural Engineering*, 15(4), 920-934, 1989.
- [18] American Association of State Highway and Transportation Officials (AASHTO), *Standard specifications for highway bridges*, 16th edition. Washington (DC), 1996.
- [19] California Department of Transportation (CALTRANS). *Memo to designers*, 20-3, 20-4. Sacramento (CA), 1994.
- [20] California Department of Transportation (CALTRANS). *Seismic Design Criteria*, 20-3, 20-4. Sacramento (CA): California Department of Transportation; 1999.
- [21] M. Tandon, Economical design of earthquake-resistant bridges, *ISET Journal of Earthquake Technology*, pp.No 453, 42(1), pp. 13-20, 2005.
- [22] J.P. Conte, Y. Zhang, Performance Based Earthquake Engineering: Application to an Actual Bridge-Foundation-Ground System, Keynote paper, *12th Italian National Conference on Earthquake Engineering*, Pisa, Italy, June 10-14, 2007.
- [23] R.A. Imbsen, AASHTO Guide Specifications for LRFD Seismic Bridge Design, Subcommittee for Seismic Effects on Bridges, *T-3, Prepared by: Imbsen Consulting*, May 2007.
- [24] A. Bozorgzadeh, S. Megally, J. Restrepo, and S. Ashford. Capacity Evaluation of Exterior Sacrificial Shear Keys of Bridge Abutments. *Journal of Bridge Engineering*, 11(5), pp. 555-565, 2006.
- [25] ENV 1992-1-1:1992 Eurocode 2: *Design of concrete structures - Part 1-1: General – Common rules for building and civil engineering structures*.